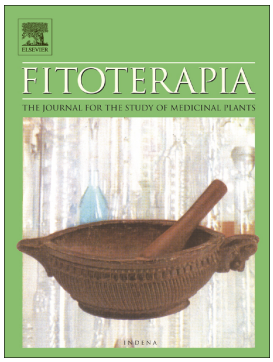

Effect of the natural polymethoxylated flavone artemetin on lipid oxidation and its impact on cancer cell viability and lipids

Antonella Rosa, Raffaella Isola, Federica Pollastro, Mariella Nieddu

PII: S0367-326X(21)00277-X

DOI: https://doi.org/10.1016/j.fitote.2021.105102

Reference: FITOTE 105102

To appear in: *Fitoterapia*

Received date: 28 September 2021

Revised date: 8 November 2021

Accepted date: 11 December 2021

Please cite this article as: A. Rosa, R. Isola, F. Pollastro, et al., Effect of the natural polymethoxylated flavone artemetin on lipid oxidation and its impact on cancer cell viability and lipids, *Fitoterapia* (2021), https://doi.org/10.1016/j.fitote.2021.105102

Effect of the natural polymethoxylated flavone artemetin on lipid oxidation and its impact on cancer cell viability and lipids

Antonella Rosa[a,*], Raffaella Isola[a], Federica Pollastro[b, c], Mariella Nieddu[a]

[a] *Department of Biomedical Sciences, University of Cagliari, Cittadella Universitaria, SS 554, Km 4.5, 09042 Monserrato, Cagliari, Italy*

[b] *Department of Pharmaceutical Sciences, University of Eastern Piedmont, Largo Donegani 2, 28100 Novara, Italy*

[c] *PlantaChem Srls, via Amico Canobio 4/6, 28100 Novara, Italy*

*Corresponding authors. Antonella Rosa, *E–mail address*: arosa@unica.it (A. Rosa), Tel.: +39 070 6754124, fax: +39 070 6754032.

ABSTRACT

The biochemical class of the polymethoxylated flavonoids represents uncommon phenolic compounds in plants presenting a more marked lipophilic behavior due to the alkylation of its hydroxylic groups. As a polymethoxylated flavone, which concerns a different bioavailability, artemetin (ART) has been examined *in vitro* against lipid oxidation and its impact on cancer cells has been explored. Despite this flavone only exerted a slight protection against *in vitro* fatty acid and cholesterol oxidative degradation, ART significantly reduced viability and modulated lipid profile in cancer Hela cells at the dose range 10-50 μM after 72 h of incubation. It induced marked changes in the monounsaturated/saturated phospholipid class, significant decreased the levels of palmitic, oleic and palmitoleic acids, maybe involving an inhibitory effect on *de novo* lipogenesis and desaturation in cancer cells. Moreover, ART compromised normal mitochondrial function, inducing a noteworthy mitochondrial membrane polarization in cancer cells. A dose-dependent absorption of ART was evidenced in HeLa cell pellets (15.2% of the applied amount at 50 μM), coupled to a marked increase in membrane fluidity, as indicate by the dose-dependent fluorescent Nile Red staining (red emissions). Our results validate the ART role as modulatory agent on cancer cell physiology, especially impacting viability, lipid metabolism, cell fluidity, and mitochondrial potential.

Keywords: Flavonoids, Lipid peroxidation, cytotoxicity, lipid profile modulation, fluidity.

1. Introduction

Flavonoids are a well-known group of polyphenolic compounds characterized by a benzo-γ-pyrone structure and occurring ubiquitously in plants and foods/beverages of natural origin [1,2]. These secondary metabolites have attracted considerable attention due to their numerous biological properties that include both pharmacological and alimentary aspects [1-6] such protecting various cell types from oxidative stress via different mechanisms [1-3], quenching radicals, chelating different ions [1,2,7], inducing cytoprotective enzymes and antioxidant transcriptional genes [3], inhibiting cancer cell viability and proliferation, angiogenesis, and migration [2,4,8]. Not negligible, cell lipid metabolism has been suggested as another possible target of dietary natural flavonoids in cancer cells [8].

An important issue is the deep correlation between the direct antioxidant potency of flavonoids and their structure that involves the number and substitutions of hydroxyl groups (Fig. 1) strongly affecting not only their free radical scavenging activity [1], but their bioavailability in terms of absorption, distribution, metabolism, and excretion [6].

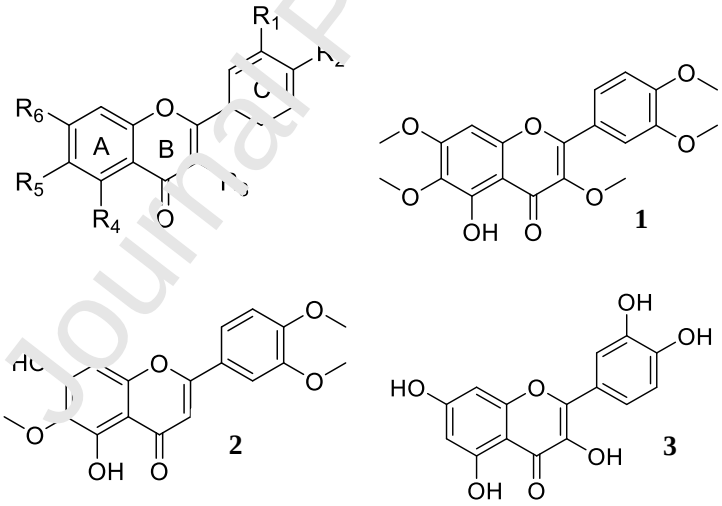

Fig. 1 General structure of flavone and chemical structures of artemetin (ART, 1), eupatilin (EUP, 2) and quercetin (QRC, 3).

Generally, flavonoids are considered to penetrate the plasma membrane both by passive diffusion and by transporters [5,6] and properties such as molecular weight and lipophilicity,

mainly established by number and type of substituents (hydroxyl, methoxyl, prenyl, and glycosyl groups), are basically involved in their absorption [5,6]. Moreover, numerous studies evidenced the ability of flavonoids to affect cell membrane fluidity and properties, interacting with the lipid membrane surface or inserting themselves into the lipid bilayer [5,9]. It has been shown that flavonoid structural properties as the partition coefficient (log P3), total number of H-bonds, and topological surface area (TPSA) [10] can reveal how these compounds penetrate cell membrane [5].

Considering all these aspects, we focused our attention on *O*-methylated flavone artemetin (5-hydroxy-3,6,7,3',4'-pentamethoxyflavone) (ART, 1) (Fig. 1) already identified as an active compound in plants and dietary spices that enjoy a long application in traditional medicine, as *Achillea millefolium* L. [11,12], *Artemisia absinthium* [12,13], *Vitex trifolia* [14], and *Artemisia argyi* [15]. ART is an uncommon polymethoxylated lipophilic flavone (log P3 = 3.4, Table 1) [10] presenting only a free hydroxyl group (in the A ring, Fig. 1) involved in a hydrogen bond with the ketone moiety, structural characteristics that could lead to substantial different biological activity.

Table 1
Properties of the tested polyphenols computed from chemical structure (form PubChem database) [10]

Phenolic compound	log P3[a]	Number of H-bonds[b]	Topological polar surface area[b]
Artemetin	3.4	9	92.7
Eupatilin	2.9	9	94.4
Quercetin	1.5	12	127.0

[a] log P3: partition coefficient for an octanol:water mixture, computed by XLogP3 3.0.

[b] computed by Cactvs 3.4.8.18.

Anyway, several studies investigated the antioxidant [12,13,16], anti-hypertensive [11], anticancer [17], antiparasitic [13], and anti-inflammatory [14,15] properties of ART, highlighting some controversial results regarding its bioactivity [13,18,19].

In this manuscript we investigated the direct ART ability to prevent the oxidative degradation of cholesterol and phospholipids, essential components of biological membranes and lipoproteins [20], which degradation plays an essential role in the development of tissue damage associated with several pathological states (inflammation, cancer, atherosclerosis, and neurodegenerative diseases) [21,22]. Moreover, experiments were designed to evidence the impact of ART on lipid

profile in cancer cells, with regard to the total fatty acid composition, phospholipids (PL) and free cholesterol (FC) levels. Lipid metabolism is considered a promising anticancer target and several antitumor drugs (lipophilic or amphiphilic molecules) act through the membranes by changing the fluidity, the general lipid membrane organization and structure, and inhibiting the expression of enzymes involved in lipid metabolism [23-27]. Changes in lipid profile in ART-treated cancer cells together with the investigation of the cell viability and the changes occurring on cell morphology, cytoplasmic membranes, and mitochondria membrane potential were investigated. Finally, the ART absorption in cancer HeLa cells was preliminary assessed. The bioactivity profile of ART was compared to that of eupatilin (EUP, 7-dihydroxy-3′,4′,6-trimethoxyflavone) (Fig. 1), a flavone analogue with antioxidant and anticancer activities, characterized by a less extent of methoxylation in the A and C rings than ART [28], in the prospective to underline structure activity relationship.

2. Experimental

2.1. Chemicals and reagents

Cholesterol, 5-cholesten-3β-ol-7-one (7-keto), 5-cholestene-3β,7β-diol (7β-OH), quercetin (QRC) (purity ≥95%), standards of fatty acids, 1,2-dipalmitoyl-*sn*-glycero-3-phosphocholine (PC 16:0/16:0), 1,2-dioleoyl-*sn*-glycero-3-phosphocholine (PC 18:1/18:1), 1-palmitoyl-2-oleoyl-*sn*-glycero-3-phosphocholine (PC16:0/18:1), 1-oleoyl-2-palmitoyl-*sn*-glycero-3-phosphocholine (PC 18:1/16:0), 2-linoleoyl-1-palmitoyl-*sn*-glycero-3-phosphocholine (PC 16:0/18:2), 2-arachidonoyl-1-palmitoyl-*sn*-glycero-3-phosphocholine (PC 16:0/20:4), 1,2-dilinoleoyl-*sn*-glycero-3-phosphocholine (PC 18:2/18:2), 1,2-dieicosapentaenoyl-*sn*-glycero-3-phosphocholine (PC 20:5/20:5), 3-(4,5-dimethylthiazol-2-yl)-2,5-diphenyltetrazolium bromide (MTT), the mixture of phospholipids (bovine brain extract, Type VII, purity > 99%), Nile Red (9-diethylamino-*5H*-benzo[a]phenoxazine-5-one) and all solvents used (purity ≥99.9%), were obtained from Sigma-Aldrich (Milan, Italy). Tetramethylrhodamine methyl ester perchlorate (TMRM) was purchased from Molecular Probes (Eugene, OR, USA). Cell culture materials were purchased from Invitrogen (Milan, Italy). All the chemicals used in this study were of analytical grade. ART was purified from aerial part of *Artemisia absinthium* collected from Orto Botanico di Guardabosone (Vercelli, Italy). A voucher specimen (OBG-2020) of the *cis*-epoxyocimene

chemotype of *A. absinthium* is stored in Novara laboratories. The reference compound EUP (with 98% purity) has been isolated from the Swiss chemotype of *Artemisia umbelliformis* Lam. (Asteraceae) according to literature [28].

2.2. Isolation of artemetin from A. absinthium

The powdered plant material of *A. absinthium* (315 g, non-woody aerial parts, leaves and flowers from the botanical garden of Guardabosone in Vercelli) was extracted with acetone (3 × 3.5 L) at room temperature, affording 20.77 g (6.6%) of a black syrup that was later purified by filtration over RP C-18 silica gel (200 g) with methanol to remove fats and pigments. The methanol filtrate was evaporated, affording 17.5 g of a brownish paste. The latter was fractionated by chromatography on silica gel (300 g, petroleum ether-ethyl acetate gradient from 90:10 to 20:80) to afford, after crystallization with diethyl ether, 504 mg (0.16%) of compound 1 (ART) (with 98% purity) as yellow powder. The compound has been identified according to literature [12,29].

2.3. Cholesterol oxidation assay

The protective effect of aliquots (1-50 nmol) of ART was evaluated during the cholesterol oxidation in dry state [25,30]. Aliquots of 0.5 mL of cholesterol solution (2 mg/mL of methanol) were dried in a round-bottom test tube under vacuum and then incubated in a bath at 140 °C for 1 h (oxidized controls) under artificial light exposure; controls (Ctrl, non-oxidized cholesterol) were kept at 0 °C in the dark. In a different set of experiments, aliquots of ART (0.5 mg/mL in methanol) solutions were added to the cholesterol solution, the mixtures cholesterol/flavone were dried under vacuum and then incubated for 1 h in dry state in a bath at 140 °C. Analyses of cholesterol, 7-ketocholesterol (7-keto), and 7β-hydroxycholesterol (7β-OH) were carried out with an Agilent Technologies 1100 liquid chromatograph equipped with a diode array detector (HPLC-DAD) as previously described [25,30].

2.4. Liposomes oxidation assay

Aliquots (300 μL) of a stock solution (1 mg/mL in chloroform) of phospholipids (PL; bovine brain extract, Type VII) were dried in a round-bottom test tube under vacuum alone or in the presence of different aliquots of ART (10, 25 and 50 μM, in methanol solution). The thin lipid

films were hydrated with saline solution (1 mg/mL solution) and the liposome dispersions (corresponding to 300 μg of lipids) were oxidized in saline solution for 24 h in the presence of 5 μM $CuSO_4$ at 37 °C in a thermostatic water bath as previously reported [25,30]. Preparation of fatty acids (FA) was obtained by mild saponification [25,30]. Analyses of unsaturated fatty acids (UFA) were carried out with an Agilent 1100 HPLC-DAD and data were collected and analyzed using the Agilent OpenLAB Chromatography data system, as previously described [25,30].

2.5. HeLa cell culture

Human adenocarcinoma HeLa cell line was obtained from the American Type Culture Collection (ATCC, Rockville, MD). Cells were grown in Dulbecco's modified Eagle's medium (DMEM) with high glucose, supplemented with 10% fetal calf serum (FCS), penicillin (100 units/mL)–streptomycin (100 μg/mL), and 2 mM L-glutamine in a 5% CO_2 incubator at 37 °C. Subcultures of the HeLa cells were grown in T-75 culture flasks and passaged with a trypsin-EDTA solution.

2.6. Cytotoxic activity in HeLa cancer cells. MTT assay

The cytotoxic effect of ART was evaluated in cancer HeLa cells by the MTT tetrazolium salt (Sigma-Aldrich, Milan, Italy) colorimetric assay [30,31]. Cancer cells were seeded in 96-well plates (at a density of 3×10^4 cells/mL and 10^4 cells/mL) in 100 μL of medium and cultured for 48 h. Cells were subsequently incubated for 24 h and 72 h with various concentrations of ART (from solutions in dimethyl sulfoxide, DMSO) in complete culture medium (treated cells). Treated cells were compared for viability to untreated cells (control cells) and vehicle-treated cells (incubated for 24 h and 72 h with an equivalent volume of DMSO; maximal final concentration, 2%). At the end of the incubation time, cells were subjected to the viability test adding 8 μL of MTT solution (5 mg/mL) as reported [30,31]. The cytotoxicity of the flavonoids QRC and EUP (from 1 mg/mL solutions in DMSO) was also tested in HeLa cells [8] for comparison at the same experimental conditions. Preliminary evaluation of the cancer cell morphology after 24 and 72 h of incubation with various amounts of ART and reference compounds was performed by microscopic analysis with a ZOE™ Fluorescent Cell Imager (Bio-Rad Laboratories, Inc., California, USA).

2.7. Lipid profile modulation in cancer HeLa cells

Cancer HeLa cells were plated in Petri dishes (at a density of 3×10^5 cells/10 mL of complete culture medium) and cultured for 48 h. Cells were subsequently incubated (at 80% of confluence) for 72 h with ART (10, 25 and 50 μM, from DMSO solutions) in complete culture medium (treated cells). Control cells (untreated cells) and vehicle-treated cells (72 h-incubation with 0.5% of DMSO) were also prepared. After different treatments, cells were washed with PBS to remove dead cells, scraped, and centrifuged (at 2000 rpm at 4 °C for 10 min). Cell pellets were separated from the supernatants and then used for the extraction of lipid compounds.

2.8. Cell lipid extraction and analysis

Total lipids were extracted from HeLa cell pellets with 6 mL of the chloroform/methanol/water 2:1:1 mixture as previously reported [25,31]. Dried aliquots of the chloroform fractions after cell pellet extraction were dissolved in methanol and injected into an Agilent Technologies 1100 HPLC system for the direct analysis of free cholesterol (FC) and phospholipids (PL). Another aliquot of dried chloroform fractions, dissolved in ethanol, was subjected to mild saponification for the analysis of cell FA as reported [25,31]. Analyses of lipid compounds were carried out with an Agilent Technologies 1100 HPLC equipped with a DAD and an Agilent Technologies Infinity 1260 evaporative light scattering detector (ELSD). PL (ELSD detection) and FC (DAD detection at 203 nm) were determined with an Inertsil ODS-2 column (Superchrom, Milan, Italy) and methanol as mobile phase at a flow rate of 2 mL/min. Analyses of unsaturated (DAD detection, 200 nm) and saturated (ELSD detection) FA, obtained from cell lipid saponification, were carried out with a mobile phase of acetonitrile/water/acetic acid (75/25/0.12, v/v/v), at a flow rate of 2.3 mL/min, and data were collected and analyzed using the Agilent OpenLAB Chromatography data system, as previously described [25,31]. Calibration curves of FA were constructed using standards and were found to be linear (DAD) and quadratic (ELSD) (correlation coefficients > 0.995) [25,31].

2.9. Analysis of ART in cancer HeLa cells

The chloroform fractions after lipid extraction from cell pellets, dissolved in methanol, were injected into the HPLC-DAD system for the analysis of ART. ART was determined with an Inertsil ODS-2 column and methanol as the mobile phase at a flow rate of 2 mL/min, detected at wavelength of 292 nm. The identification of ART in cell extracts was made using standard

compound, conventional UV spectra and literature UV data [32]. Calibration curve was constructed using ART standard and was found to be linear (correlation coefficients > 0.998).

2.10. Fluorescence microscopy

Fluorescent microscopy studies were performed on 35 mm Petri dishes, where HeLa cells were seeded until they reached 80% confluence. To check ART impact on cytoplasmic membranes [8,31], cells were stained with 300 nM Nile Red (NR), as NR red fluorescence, corresponds to cytoplasmic membranes. To evaluate ART effect on mitochondrial potential cells were treated with 50 nM TMRM (tetramethylrhodamine methyl ester). TMRM fluorescence, indicating mitochondrial potential [25] was acquired with 546±6 excitation filter and 620±60 emission filter. Both treatments with fluorophores were in DMEM without serum in a CO_2 incubator for 45 min. Prior observation, dyes were washed out from Petri dishes to avoid background fluorescence. HeLa cells were observed under a Zeiss Axioskop upright fluorescence microscope (Zeiss, Jena, Germany), equipped with 10×, 20× and 40×/0.75 NA water immersion objectives. and. Fluorescence images were acquired with a cooled CCD camera (QICAM, Qimaging, Canada). Image analysis of TMRM images was performed with Image J and Image Pro Plus (Media Cybernetics, Silver Springs, MD). Briefly, background fluorescence was subtracted from images and histogram values of mean fluorescence intensity were normalized per cell number. Per each ART dose and control samples 5-6 images were acquired with an objective 20× (embracing 20-80 cells each) and processed for image analysis. Data were then processed as percentages of controls.

2.11. Statistical analyses

All data were preliminary assessed for normal distribution with Graph Pad INSTAT software. Evaluation of the statistical significance of differences was then performed using one-way analysis of variation (One-way ANOVA), followed by the Bonferroni post hoc Test or Holm-Sidak post-hoc test with Graph Pad INSTAT software (GraphPad software, San Diego, CA) and Sigma-Plot software (Systat INC, Delaware, US). Results were expressed as mean ± standard deviation (SD) or standard error of the mean (SEM), and statistically significant differences was evaluated with $P < 0.05$ as a minimal level of significance.

3. Results

3.1. Protective effect against cholesterol oxidation

The antioxidant activity of ART was assessed during cholesterol oxidation in dry state at 140 °C for 1 h [8,30]. The decrease of the cholesterol level (at 140 °C, cholesterol was an oil) and the formation of the oxidized products 7-keto and 7β-OH were measured as markers of the oxidative process in the absence or in the presence of ART. Fig. 2A shows the antioxidant activity, expressed as % of protection, of different amounts (1-50 nmol) of ART during cholesterol degradation. Values (μg) of oxysterols (7β-OH and 7-keto) measured in the control (Ctrl, at 0 °C) and in the absence (0, oxidized control) or in the presence of ART are also reported in Fig. 2B.

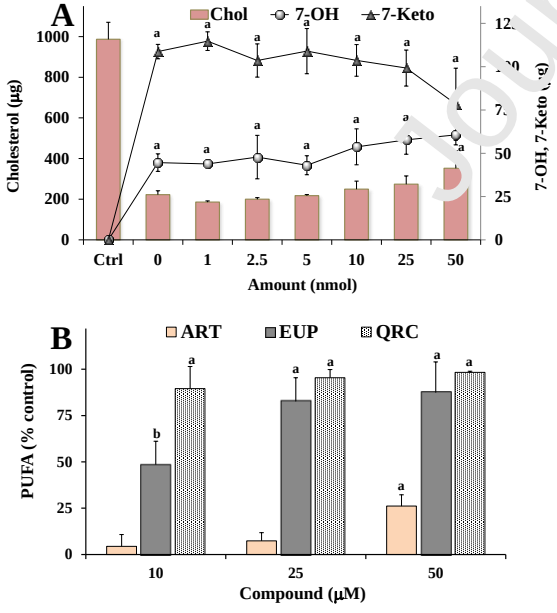

Fig. 2 (**A**) Values (μg) of cholesterol and oxysterols (7β-OH and 7-keto) measured in the control (Ctrl) and in the absence (0, oxidized control) and in the presence of different aliquots (1-50 nmol) of artemetin (ART) during cholesterol oxidation at 140 °C for 1 h; a = $p < 0.001$

versus oxidized control (0). (**B**) Antioxidant activity, expressed as % protection, of different amounts (1-50 nmol) of ART, eupatilin (EUP) and quercetin (QRC) measured during cholesterol oxidation at 140 °C for 1 h; a = $p < 0.001$, b = $p < 0.01$ versus oxidised control (0% protection). Three independent experiments are performed, and data are presented as mean and SD (n = 6). Statistical significance of differences was performed using One-way ANOVA and the Bonferroni post Test.

The protective effect of QRC and EUP, previously tested in the same experimental conditions [8], is reported in Fig. 2B for comparison. In this system ART showed a low potency in protecting cholesterol from degradation, exerting a significant 26% protection only at 50 nmol, without reducing 7-keto and 7β-OH formation with respect to oxidized control at all tested concentrations. On the contrary, EUP and QRC exerted a significant protection of the thermal-induced cholesterol decrease at almost all the tested concentrations, reducing the oxysterol formation [8].

3.2. Protective effect against liposome oxidation

The protective effect of ART was then evaluated versus the liposome oxidative injury. Liposomes were treated with Cu^{2+} ions for 24 h at 37 °C and the variation of unsaturated fatty acid (UFA) levels was analysed as an index of the lipid peroxidation process. Fig. 3 shows the total values of the main polyunsaturated FA (arachidonic acid, 20:4 n-6; docosatetraenoic acid, 22:4 n-6; docosahexaenoic acid 22:6 n-3) (PUFA) (expressed as % of the control) measured in the control (Ctrl) and during Cu^{2+}-induced liposome oxidation in the absence (0, oxidized control) and in the presence of different concentrations (10, 25 and 50 μM) of ART (Fig. 3) and the reference phenols QRC and EUP [8].

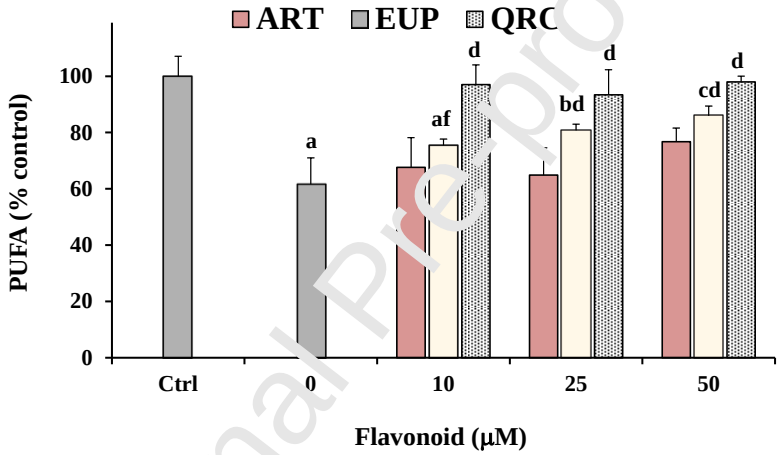

Fig. 3 Total values of the polyunsaturated fatty acids (PUFA), as sum of 20:4 n-6, 22:4 n-6 and 22:6 n-3, expressed as % control, measured in control (Ctrl) and during liposome oxidation at 37 °C for 24 h with 5 mM $CuSO_4$ in the absence (oxidized control, 0) or in the presence of different amounts of artemetin (ART), eupatilin (EUP) and quercetin (QRC). Three independent experiments are performed, and data are presented as mean ± SD (n = 6); a = $p < 0.001$, b= $p < 0.01$, c= $p < 0.05$ versus Ctrl; d = $p < 0.001$, f = $p < 0.05$ versus 0 (One-way ANOVA and Bonferroni post Test).

A strong and significant decrease (40%) of PUFA level was observed after 24 h oxidation in oxidized control. ART did not show a significant antioxidant activity against PUFA consumption at all tested concentrations. On the contrary, QRC and EUP, previously assayed in this oxidative stress system [8], showed at the tested concentrations an antioxidant protection in the 92-97% and 36-64% range for EUP and QRC, respectively.

3.3. Cytotoxicity on cancer HeLa cells

The cytotoxic effect of ART was investigated on HeLa cells, a cell line derived from a human cervical epithelioid carcinoma. Fig. 4A shows the viability, expressed as % of the control, induced by incubation for 24 h with different amounts (0.5-200 μM) of ART and the reference compounds QRC and EUP [8] in cancer HeLa cells by MTT assay.

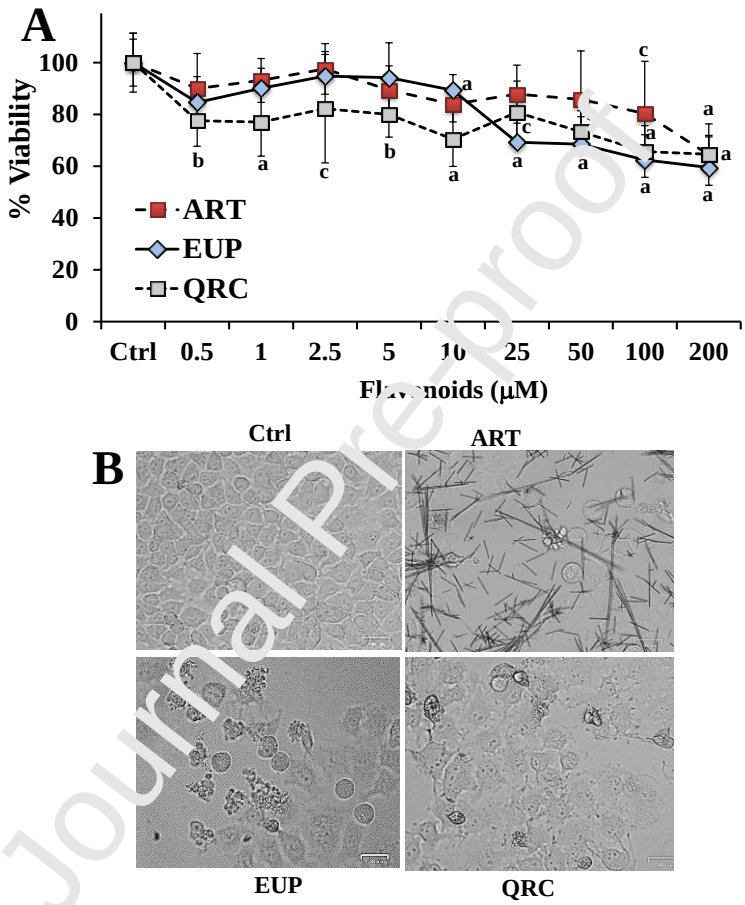

Fig. 4 (**A**) Viability, expressed as % of the control (Ctrl), induced by incubation for 24 h with different amounts (0.5-200 μM) of artemetin (ART), eupatilin (EUP) and quercetin (QRC) in cancer HeLa cells (MTT assay). Three independent experiments are performed, and data are presented as mean ± SD (n = 12); a = p< 0.001, b = p< 0.01, c = p< 0.05 versus Ctrl (One-way ANOVA and Bonferroni post Test). (**B**) The panel shows representative images of phase contrast of control HeLa cells and cells treated for 24 h with 200 μM of the three flavonoids. Bar = 30 μm.

ART was not significantly toxic at the dose range of 0.5-50 μM, whereas exerted a significant reduction in HeLa cell viability, in comparison with control cells, from the dose of 100 μM (with a viability reduction of 20%). A significant cancer cell growth inhibition (reduction of viability: 36%) was observed at the dose of 200 μM. An analogous treatment with QRC and EUP induced a major decrease in cancer cell viability at lower doses than ART, whereas similar values of viability reduction were observed for all the flavonoids at 200 μM. DMSO, used to dissolve flavonoids, was not toxic in HeLa cancer cells and cell viability, measured at the maximal tested dose (2%), was 92%. The preliminary microscopic observation of ART-treated cells before MTT assay (Fig. 4B), allowed us to evidence different cell morphologies in HeLa cells after 24 h-incubation at the highest tested doses, however a marked drug precipitation in form of crystals was observed. Therefore, to avoid the effects of precipitation, ART cytotoxicity was tested at lower amounts for a longer incubation time (72 h). Fig. 5A shows the viability (as % control) of HeLa cells after 72 h of incubation with different amounts of ART (0.5-50 μM) and the reference

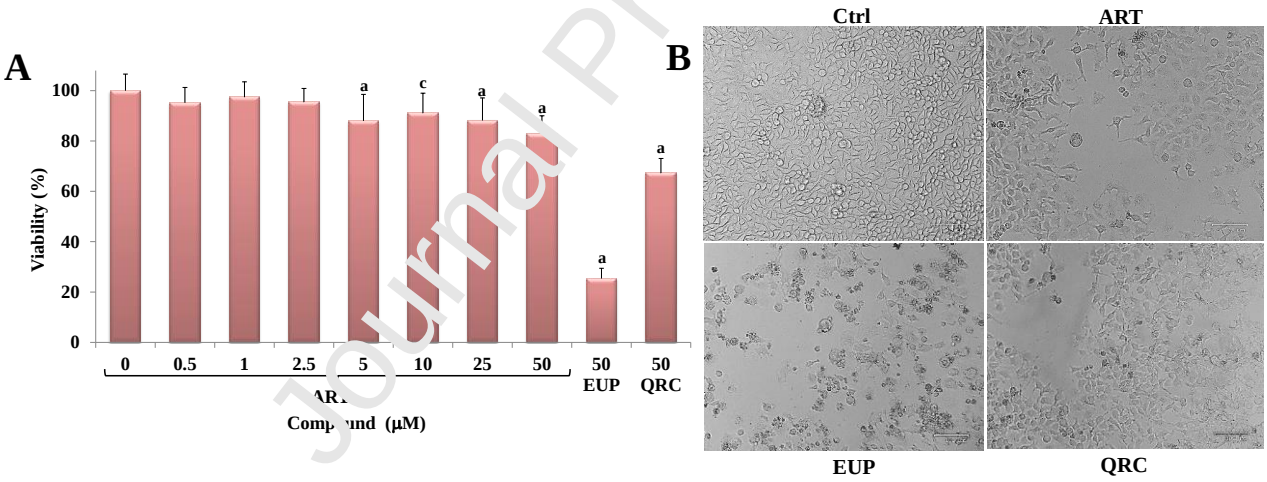

compounds QRC (50 μM) and EUP (50 μM) by MTT assay.

Fig. 5 (**A**) Viability, expressed as % of the control (Ctrl), induced by incubation for 72 h with different amounts (0.5-50 μM) of artemetin (ART) in cancer HeLa cells (MTT assay). The effect of eupatilin (EUP) and quercetin (QRC) at the dose of 50 μM on HeLa viability after 72 h-incubation is reported for comparison. Three independent experiments are performed, and data are presented as mean and SD (n = 12); a = $p < 0.001$, c = $p < 0.05$ versus Ctrl (One-way ANOVA and Bonferroni post Test). (**B**) The panel shows

representative images of phase contrast of control HeLa cells and cells treated for 72 h with the three flavonoids at 50 μM. Bar = 100 μm.

A significant reduction of viability compared to controls, ranging from 12 to 18%, was observed for ART from the dose of 5 μM to 50 μM. At 50 μM, QRC and EUP were more toxic than ART, inducing a statistically significant viability reduction of 33% and 75%, respectively, when compared to controls. DMSO, used to dissolve the flavonoids, was not toxic in HeLa cancer cells and cell viability, measured at the maximal tested dose (0.5%), was 95%. Phase contrast images of HeLa cells after 72 h-treatment (Fig. 5B) with the dose of 50 μM of flavonoids showed less marked changes in the cell morphology of ART-treated cells than those treated with QRC and EUP.

3.4. Lipid profile modulation in cancer HeLa cells

ART then tested in cancer HeLa cells to assess its effects after 72 h-incubation on cancer cell lipid composition (main polar lipid classes and total FA profile). Fig. 6 shows the chromatographic profiles (Fig. 6A) and % area values (Fig. 6B) of polar lipid compounds, mainly constituted by phospholipids (PL) and free cholesterol (FC), of HeLa control cells and cells treated for 72 h with ART (at 10, 25 and 50 μM) obtained by HPLC-ELSD analysis.

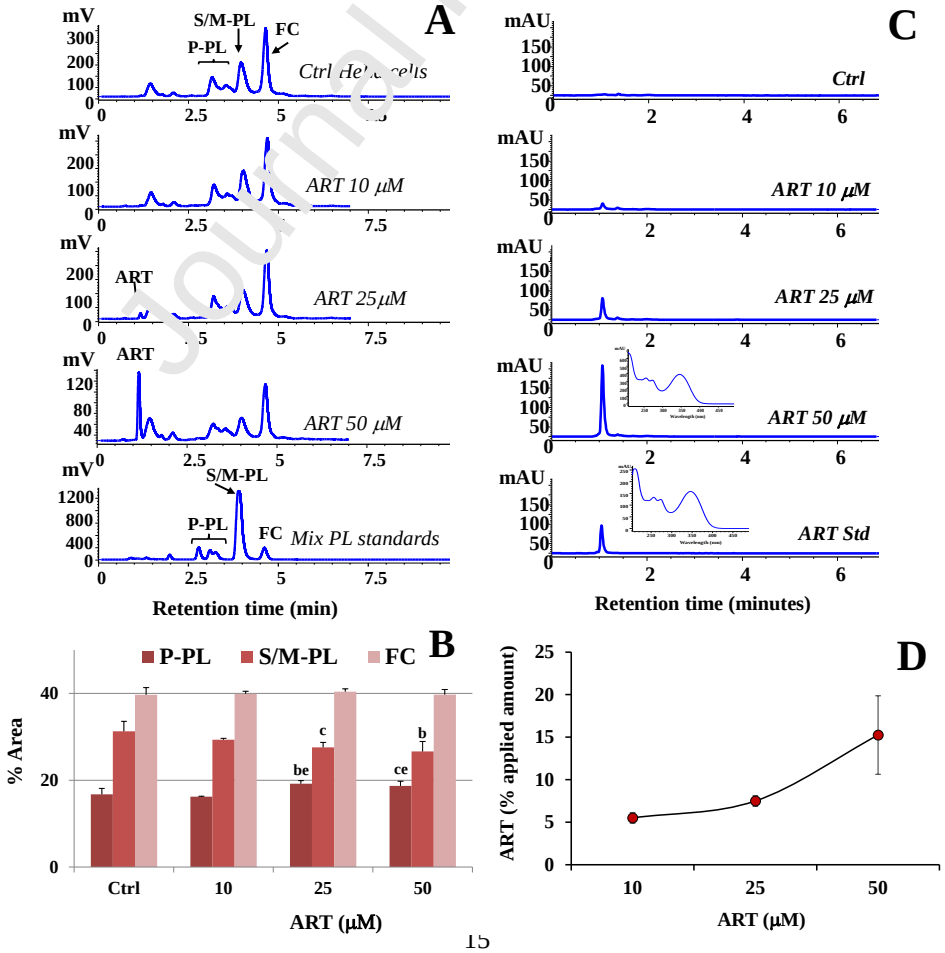
A
mV
S/M-PL
P-PL
FC
Ctrl HepG2 cells
ART 10 μM
ART
ART 25μM
ART 50 μM
Mix PL standards
Retention time (min)
C
mAU
Ctrl
ART 10 μM
ART 25 μM
ART 50 μM
ART Std
Retention time (minutes)
B
P-PL
S/M-PL
FC
% Area
be
c
ce
b
Ctrl
10
25
50
ART (μM)
D
ART (% applied amount)
ART (μM)

Fig. 6 (A)

Chromatographic profile (obtained by HPLC-ELSD analysis) of saturated/monounsaturated phospholipids (S/M–PL), polyunsaturated phospholipids (P-PL) and free cholesterol (FC), measured in control HeLa cells (Ctrl) and cells treated for 72 h with different amounts (10, 25 and 50 μM) of artemetin (ART). The chromatographic region for each lipid class was assigned by using standard mixtures of saturated/monounsaturated (mix PL: PC 16:0/16:0, PC 18:1/18:1, PC 16:0/18:1, PC 18:1/16:0, ECN 32) and polyunsaturated phosphatidylcholines (PC 16:0/18:2, ECN 30; PC 16:0/20:4, PC 18:2/18:2, ECN 28; PC 20:5/20:5, ECN 20). (**B**) Values (% area) of S/M–PL, P–PL, and FC measured in control and ART-treated HeLa cells. Results were expressed as a mean ± standard deviation (SD) of three independent experiments; a = $p < 0.001$ versus Ctrl (One-way ANOVA and Bonferroni post Test). (**C**) Chromatographic profiles and UV spectra (292 nm) of peaks measured in the chloroform fractions obtained from control HeLa cells and cells treated with different doses of ART. ART in cell extracts was identified by comparison with the retention time and spectrum of ART standard. (D) Values of ART (expressed as % of applied amount) measured in HeLa cell pellets after 72 h-incubation with the flavone. Results were expressed as a mean ± standard deviation (SD) of two independent experiments; a = $p < 0.001$ versus 10 μM (One-way ANOVA and Bonferroni post Test).

In our experimental conditions, control HeLa cells showed a polar lipid profile characterized by a peak of FC and two main peaks of PL, corresponding to saturated/monounsaturated PL (S/M-PL) and polyunsaturated PL (P-PL). The chromatographic region for each lipid class was assigned by using standard mixtures of saturated, monounsaturated (S/M-PL) and polyunsaturated (P-PL) phosphatidylcholines, and FC as previously reported [25,31]. Cell polar lipids were separated on the basis of ECN (=CN−2n, where CN is the number of acyl group carbons and n the number of double bonds) [25,31]. ART-treated cells showed a dose-dependent change in the lipid profile with respect to control cells, with a significant decrease in the peak area of S/M-PL from 25 μM ($p < 0.05$ versus untreated cells) and a significant increase in the % of P-PL versus untreated cells ($p < 0.05$).

Fig. 7 shows values of fatty acids (FA) (Fig. 7A) and total amounts of saturated (SFA), monounsaturated (MUFA), and polyunsaturated (PUFA) FA (Fig. 7B) (expressed as μg/plate) measured in control HeLa cells and cells incubated for 72 h in the presence of different amounts of ART (10, 25 and 50 μM).

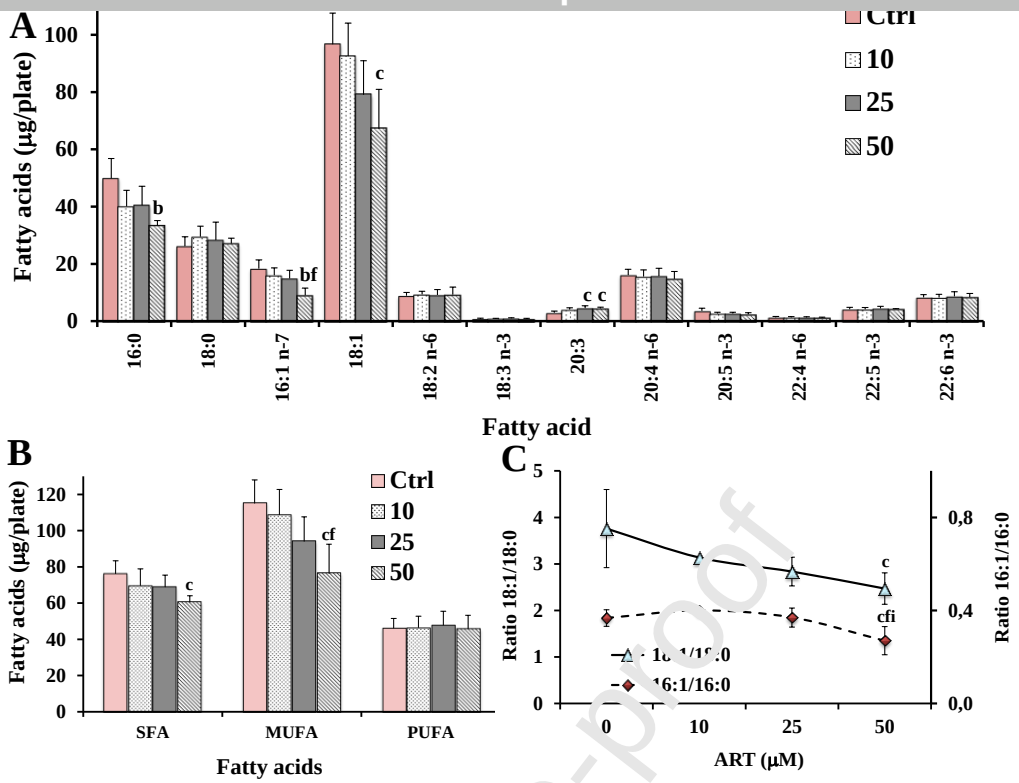

Fig. 7 (**A**) Values (expressed as µg/plate) of the main fatty acids (**A**), total saturated (SFA), monounsaturated (MUFA), polyunsaturated (PUFA) fatty acids **(B**), and values of the ratios 18:1 n-9/18:0 and 16:1 n-7/16:0 (**C**) measured in control HeLa cells and cells treated for 72 h with different amounts (10, 25 and 50 µM) of artemetin (ART). Three independent experiments with two replicates for each condition are performed and data are presented as mean ± SD (n = 6). b = $p < 0.01$, c = $p < 0.05$ versus Ctrl; f = $p < 0.05$ versus ART 10 µM; i = $p < 0.05$ versus ART 25 µM (One-way ANOVA and Bonferroni post Test).

Control HeLa cells showed a FA composition characterized by a high level of 18:1 isomers (96.7 ± 10.9 µg/plate, 41% of TFA; mainly 18:1 n-9), 16:0 (49.9 ± 6.9 µg/plate, 21%), stearic acid 18:0 (26.2 ± 3.2 µg/plate, 11%), and palmitoleic acid 16:1 n-7 (18.3 ± 3.0 µg/plate, 8%), while 20:4 n-6 (16.1 ± 2.0 µg/plate, 7%) represented the most abundant FA among polyunsaturated FA (PUFA), followed by docosahexaenoic acid 22:6 n-3 (8.3 ± 0.9 µg/plate, 4%). The incubation of cancer HeLa cells with ART induced marked changes in the FA profile with respect to untreated-control cells (Fig. 7A and 7B). ART induced a dose-response decrease in the cell level of MUFA ($p < 0.05$ versus controls at 50 µM). In particular, 18:1 isomers (mainly constituted by oleic acid, 18:1 n-9) and palmitoleic acid (16:1 n-7) significantly

decreased in ART-treated cells, together with a decrease in the level of palmitic acid 16:0, whereas PUFA levels in ART-treated HeLa cells were similar to controls. The 18:1 n-9/18:0 ratio value (Fig. 7C) noticeably decreased in ART-treated cells with respect to untreated-control cells ($p < 0.05$ at 50 μM), and a reduction was observed also in the 16:1 n-7/16:0 ratio value at ART 50 μM. A marked decrease in the MUFA/PUFA ratio was observed in 50 μM ART-treated cells (1.7 ± 0.1) compared to control cells (2.5 ± 0.1). Cells treated with DMSO, used to dissolve all compounds, did not show differences in the FA levels with respect to controls.

By HPLC, the FC level was measured in HeLa control cells as a mean content of 54.3 ± 4.5 μg per plate, with a total FA (TFA)/FC ratio value of 4.0 ± 0.6. The 72 h-incubation with ART did not induce in treated cells a reduction in the TFA/FC ratio, with a value of 4.0 ± 0.3 at EUP 50 μM.

3.5. ART determination in HeLa cell pellets

A preliminary study was performed to determine the ART absorption in HeLa cells. Fig. 6C show the chromatographic profiles and UV spectra (at the wavelength of 292 nm) of peaks measured in the chloroform fractions obtained from control HeLa cells and cells treated for 72 h with different doses (10, 25, and 50 μM) of ART. The presence of flavone in cell extracts was assessed by comparison with the retention time and spectrum of the ART standard. A dose-dependent increase of the ART level was evidenced in HeLa cell pellets (Fig. 6D) and values of 7.5 ± 0.6 μg/plate and 15.2 ± 1.6 μg/plate (corresponding approximately to 7.5% and 15.2% of the applied amount) of ART were measured in cell HeLa pellets after 72 h of incubation with ART 25 μM and 50 μM, respectively.

3.6. Effect on cell membranes and mitochondrial potential

Fig. 8A shows representative images of phase contrast and red emission of control HeLa cells and cells treated for 72 h with 10, 25 and 50 μM ART. Nile red (NR) is a fluorescent lipophilic dye used for the detection of lipids, characterized by a shift of emission from red to green according to the degree of hydrophobicity of the bound lipid [25,32]. In particular NR bears an intense red emission in the presence of polar PL, which constitute the plasma and intracellular membranes of organelles such as peroxisomes, lysosomes, endosomes, Golgi apparatus, endoplasmic reticulum, and mitochondria [25,32]. Seventy-two hours treatment with all ART

tested concentrations resulted in a significant increase of the red emission in NR-loaded cells (Fig. 8A, third column).

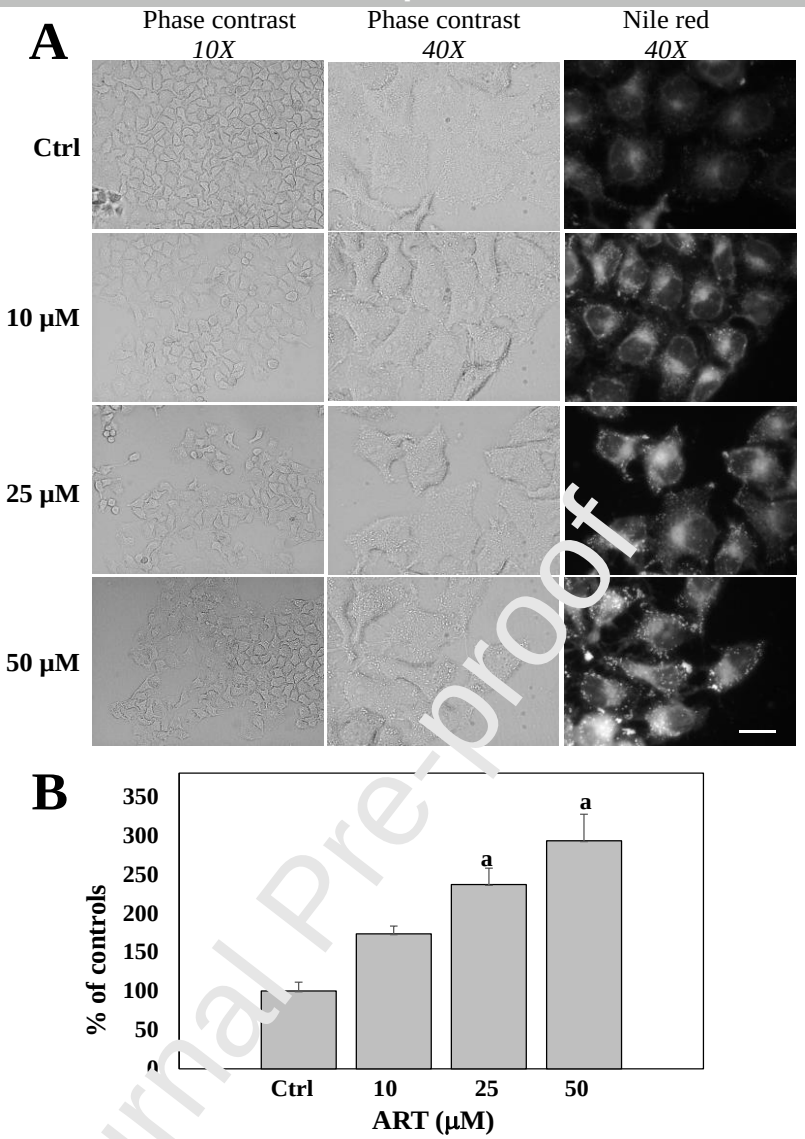

Fig. 8 (**A**) Representative images of HeLa cells by phase contrast and fluorescence microscopy observation. Control cells (Ctrl) and cells treated for 72 h with 10, 25 or 50 µM ART were stained with Nile Red (NR) and their red emission was acquired as corresponding to cell membranes. (B) NR quantification of cytoplasmic membranes (red emission) after ART treatment (10, 25 or 50 µM for 72 h). Data are expressed as percent of Ctrl ± SEM. a = $p < 0.001$ versus Ctrl (One-way ANOVA and Holm-Sidak post hoc test). Bar = 50 µm.

Quantitative fluorescent measurements (expressed as % of controls) performed on whole cells (Fig. 8B) highlighted a noticeably significant dose-dependent increase in the levels of NR red emissions compared to the untreated cells, with an increase of 300% at 50 μM. Cells treated with DMSO, used to dissolve the compound, did not show differences in their levels of NR red emissions with respect to the control (data not shown). Phase contrast images show that control HeLa cells were small, packed, and mononucleated with a bright fluorescence corresponding to their inner cell membranes, as previously reported [8]. No noticeable changes in morphology were observed in ART-treated cells at all tested doses.

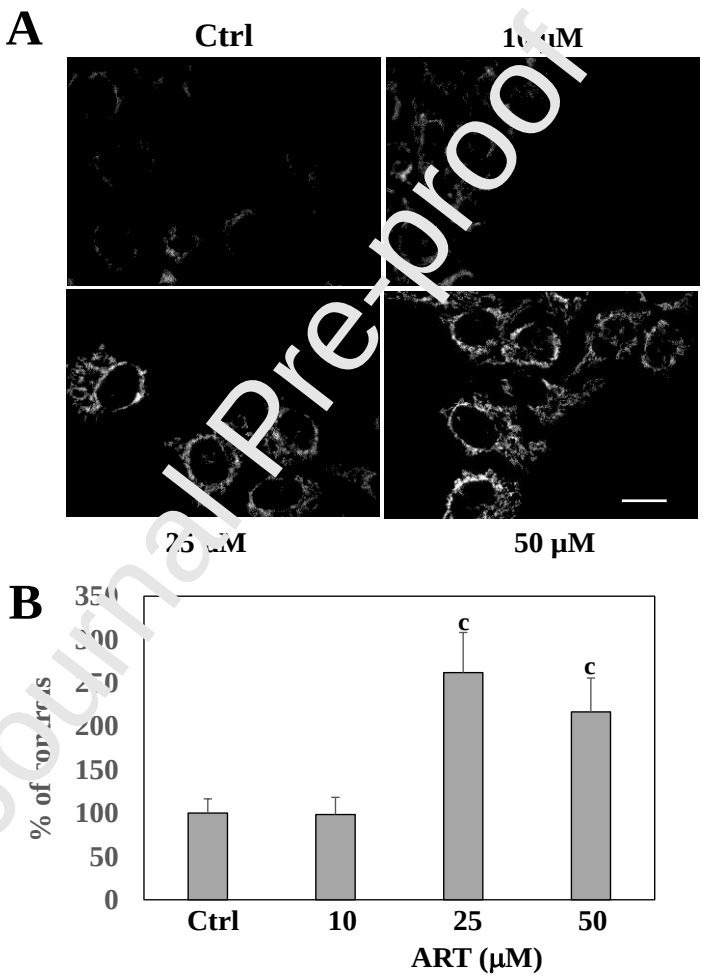

HeLa cells were also loaded with TMRM, a potential-sensitive probe that accumulates in active mitochondria according to their membrane potential [8,25,33] in order to explore the effects of ART on mitochondria physiology of cancer cells. Fig. 9 shows the mitochondrial potentials of HeLa control cells and cells treated for 72 h with 10, 25 and 50 μM ART (Fig. 9A).

Fig. 9 (**A**) Mitochondrial potential as revealed by TMRM on control HeLa cells (Ctrl) and after artemetin (ART) treatment (10, 25 and 50 μM) for 72 h. (**B**) ART treatment increased mitochondrial potential from the tested dose of 25 μM. Data are expressed as percent of Ctrl and SEM. c = $p < 0.05$ versus Ctrl (One-way ANOVA and Holm-Sidak post hoc test). Bar = 50 μm.

TMRM quantification of mitochondrial potential variations (expressed as % of control cells) (Fig. 9B) showed that ART treatment significantly increased the mitochondrial potential from 25 μM, with values of 267% and 217%, compared to the Ctrl cells ($p < 0.05$), at 25 and 50 μM, respectively.

4. Discussion

Between the biochemical class of flavonoids, ART has been shown to exert a broad-spectrum activity. ART is an uncommon flavonoid which polymethoxylation characterizes a high hydrophobicity, as indicated by its structural characteristics such as the partition coefficient (log P3) for the octanol:water mixture, the number of H-bonds formed, and the topological polar surface area (TPSA), as given in Table 1 [10].

The ART direct antioxidant activity was evaluated against the oxidative degradation of cholesterol in dry state (at 140 °C) and Cu^{2+} ions-induced liposome oxidation (at 37 °C), *in vitro* models amply validated on natural compounds [8,25,30]. In our study ART, in dry state at the

tested dose range, was devoid of a noticeable protective effect against cholesterol oxidation, without preserving from the formation of its oxidative products (oxysterols) exerting a key role in the development of tissue damage and pathological events [34]. In our cholesterol oxidation assay, the antioxidant potency of a compound depends on the ability to scavenge lipoperoxyl ($LOO^{\bullet}$) radicals, strictly correlated to the presence (number and positions) of hydrogen donating substituents like phenolic hydroxyl groups, lipophilicity, and thermal stability, as previously demonstrated [8,25,30]. ART is a lipophilic flavonoid with one hydroxylic group in its molecular structure (ring A) closed to a ketone group and probably involved in a hydrogen bond. In this system, the lack of a direct $LOO^{\bullet}$ radical scavenging activity of ART is ascribable to the quite totally absence of H-donating hydroxyl groups. The role of hydroxyl groups in the antioxidant protection against cholesterol degradation is well characterized by the strong $LOO^{\bullet}$ radical scavenging activity of the reference compounds EUP and QRC, due to their ability to donate H-atoms from their phenolic functional groups (acting as chain-breaking antioxidants) [80]. EUP has two hydroxyl groups in the ring A, while QRC is the most famous antioxidant flavonoid, bearing a catechol ring B linked in position 2 to the polyhydroxylated chromen-4-one core, previously demonstrated as the "active" moiety that scavenges LOO• radicals by formal H-atom transfer [35].

Numerous studies have been carried out to understand the role of lipid oxidation in phospholipid membranes [36]. Liposomes are considered an important membrane model useful to assess the antioxidant properties of phenolic compounds [8,9,30] and to predict the ability of flavonoids to interact with cell membrane in relation to their lipophilicity [5,9]. The antioxidant activity of a compound in our system has been related to a direct $LOO^{\bullet}$ scavenging activity and Cu^{2+} ion chelation ability [8,25,30]. ART, unlike EUP and QRC, showed no ability to protect liposomes against copper-induced oxidation. Again, the failure of ART in free radical scavenging against liposome membrane peroxidation may be due to its scarcity of H-donating substituents and its high lipophilicity (high log P3 value) (Table 1), which may influence the compartmentalization of ART into the lipid bilayer [5]. On the contrary, the powerful antioxidant activities of EUP and QRC against phospholipid membrane oxidation have been related to direct $LOO^{\bullet}$ scavenging activity (mediated by H-donating properties) and Cu^{2+} chelation activity at/near the phospholipid surface [8]. Our results showed that ART does not act as a direct inhibitor of lipid peroxidation in biological *in vitro* systems. Previous studies evidenced the ability of ART to

scavenge free radicals generated in CCl_4-intoxicated livers of rats [16] and peroxyl radicals generated from thermal homolysis of 2,2′-azobis-amidinopropane (by total oxyradical scavenging capacity assay) [37]. In contrast, ART displayed low antioxidant activity in DPPH (1,1-diphenyl-2-picrylhydrazyl) radical scavenging assay [13,38], with a SC_{50} value (concentration required to scavenge 50% of DPPH radicals) exceeding 500 μM [38].

Deregulation of lipid metabolism is one of the most important metabolic hallmarks of cancer cells and targeting lipid metabolism (fatty-acid biosynthesis and desaturation, phospholipids and cholesterol metabolism, lipid droplet synthesis) is a promising therapeutic strategy for human cancer [39-41]. The antitumor property of ART has been associated to its ability to modulate a variety molecular targets and signaling pathways in different cancer cell types, inducing cytotoxic [17,42] and antiproliferative effects [43,44], apoptosis [43,45], and cell circle arrest at G2/M phase [46]. We studied, for the first time, the impact of this natural dietary compound on cell lipids in HeLa cells, a cancer cell line derived from a human cervical epithelioid carcinoma, widely used as a model for oncological studies [8]. At first, a set of experiments was performed to assess ART cytotoxicity in cancer HeLa cells. ART, like the well-known anticancer flavonoids EUP [8] and QRC [47] significantly reduced viability (36%) in HeLa cells at 200 μM after 24 h-incubation. However, the low solubility of ART in cell medium from a concentration of 100 μM, prompted us to evaluate cytotoxicity at low doses for a long incubation time. The significant viability reduction (18%) observed at 50 μM after 72 h of incubation was comparable to values previously observed in human hepatocellular carcinoma (HepG2) and human neuroblastoma (SH-SY5Y) cells after 72 h of incubation with the same dose of ART [17]. A viability reduction of 20% was observed in human gastric cancer (AGS) cells and human breast cancer (MCF-7) cells by MTT assay after 24 h-incubation with ART (IC_{50} > 50 μM) [45], whereas an IC_{50} value of 31 μM was reported for 96 h-incubation with the compound [43]. Microscopic observation did not show evident changes in the cell morphology of HeLa cells treated with ART 50 μM for 72 h with respect to untreated cells, and no evident signs of apoptotic process were detected. At this treatment condition, EUP and QRC showed higher cytotoxicity than ART, inducing marked apoptotic morphology in HeLa cells, as previously reported [8,47].

HeLa cell treatment with ART for 72 h induced marked changes in lipid composition and this effect was evident from the lowest tested concentration. ART significantly modulated FA and PL profiles in HeLa cells, with a marked reduction in the levels of 16:0, 18:1 n-9 and 16:1 n-7, and a

decrease in the amount of S/M-PL coupled to an increase in the P-PL value. Phosphatidylcholines (PC) represent the predominant polar lipid class (53%) in HeLa cell membranes and PC 16:0/18:1 (approx. 28%) are the dominant PC, followed by PC18:1/18:1 and PC16:0/16:1 [48]. Therefore, the decrease in the S/M-PL level was principally due to the reduction of PL containing 16:0, 18:1 n-9 and 16:1 n-7. Fatty acid synthase (FAS) is a multi-enzyme that catalyzes *de novo* synthesis of palmitic acid and many anticancer flavonoids, like lutein, quercetin and amentoflavone, are FAS inhibitors [27,40]. The reduction of palmitic acid induced by ART in cancer HeLa cells was compatible with a potential inhibition of FAS. In addition, the reduction of 18:1 n-9 and 16:1 n-7 observed in ART-treated cells was compatible with a potential inhibition of the stearoyl-CoA desaturase (SCD), an enzyme that inserts a double bond in the Δ^9 position of SFA (16:0 and 18:0) to generate MUFA (16:1 n-7 and 18:1 n-9) [26,40,49]. *De novo* synthesis of UFA is often required by cancer cell lines to generate membranes and maintain membrane fluidity, essential to cell proliferation [49]. Oleic acid, the main product of SCD, is essential for the generation of complex lipids (phospholipids, triglycerides, and cholesterol esters) [40]. Therefore, inhibition of SCD leads to UFA depletion and influences the phospholipid composition of cellular membranes, consequently affecting membrane properties [26]. ART showed the ability to modulate the FA profile in cancer HeLa cells after 72 h of incubation, maybe reducing lipogenesis and affecting FA desaturation and the biosynthesis of PL, that represent building blocks for biological membranes. A general increase in the % level of cell PUFA and PL containing PUFA was observed after ART treatment. Moreover, a marked decrease in the MUFA/PUFA ratio was observed in ART-treated cells compared to control cells. However, incubation with ART did not lead to changes in the cell ratio of SFA to MUFA. Similar modifications in the FA composition (reduction of 16:0 and 18:1 n-9 and accumulation of 18:0) and PL (decrease in the % of S/M-PL) were previously observed for the flavone EUP in cancer HeLa cells at the same doses after a low incubation time (24 h) [8]. In cancer cells, changes in lipid components severely affect functional and biophysical properties of cytoplasmic and organelle membranes (changes in membrane organization, structure, and fluidity), perturbing membrane lipid raft and consequently protein dynamics [26,27,40]. The maintenance of physiological cell membrane fluidity is a prerequisite for proper membrane function and associated with cell viability and normal cell growth and division [50].

Interestingly, a significant increase in the fluorescent intensity after NR staining (red emission) was observed in ART-treated cells, indicating changes occurring on their cytoplasmic membranes [8,25,31]. NR is an uncharged fluorescent dye that partitions into lipid membranes based on its intrinsic hydrophobicity, and its fluorescence is sensitive to physical changes in its lipid environment [33,51]. The fluidity of membranes is known to influence the fluorescent staining of NR, and previous studies demonstrated that an increase/decrease in membrane fluidity due to changes in cell growth temperature leads to a corresponding increase/decrease in NR fluorescence [51]. It has been proved that flavonoids possess the ability to localize either in the hydrophobic core of the membrane lipid bilayer or at the cell lipid membrane surface, leading to corresponding alterations in the membrane fluidity or rigidity in relation to their chemical properties and hydrophobicity [5,9,52]. Partition coefficient (log P) provides information on the hydrophobicity of a molecule; in general, if the value of log P is greater than 1, the molecule is considered to possess a hydrophobic nature [52]. For flavonoids, log P value has been correlated with the extent of their interaction with biological membranes [5,52]. The inverse correlation between the number of hydroxyl groups and the lipophilicity of flavonoids has been demonstrated experimentally [7]. The membrane rigidifying effects of dietary flavonoids is one of the key factors for their anti-cancer activity and this phenomenon exhibits a dose dependency [52]. Flavonoids can penetrate into the hydrophobic and interphase sites of biological membranes like lipid rafts [7]. Furthermore, the membrane interactions and localization of flavonoids is fundamental in altering membrane-mediated cell signaling pathways [52]. The influence of flavonoids on the physical properties of the lipid bilayer may control the arrangement of membrane proteins and the formation of functional complexes responsible for cell signal transduction and the regulation of the metabolism [7]. It is well known that cancer cells rearrange lipid composition/organization to avoid apoptosis and resist to anticancer drugs [53]. The lipophilic nature of ART (log P = 3.4) could be probably responsible for a direct insertion of this flavone into the cytoplasmic membranes, inducing a decrease in the cell membrane fluidity. Thus, the change in the lipid composition (% increase of PUFA and PL containing PUFA) observed in ART-treated HeLa cells after 72 h-incubation may be an adaptive strategy of cancer cells to increase their membrane fluidity in the presence of a rigidifying agent.

The ability of ART to interact with cell membranes was also confirmed by the dose-dependent increase of this phenol in the cell pellets (15.2% of the ART applied amount was measured in cell

HeLa after 72 h of incubation at 50 μM). NR fluorescence is sensitive to the polarity of its environment, therefore, the increase in the red fluorescence intensity (cytoplasmic membranes) observed in ART-treated cells may be due to their higher cell membrane fluidity with respect to non-treated cells, as consequence of changes in cell lipid composition to counteract membrane rigidity induced by ART.

Changes occurring on mitochondria membrane potential were also investigated in ART-treated cancer cells. Our data disclosed a significant increase ($p < 0.05$ versus control cells) of the mitochondrial membrane potential after 72-h incubation of HeLa cells from ART 25 μM. The increase of mitochondrial potential is indicative of an effect of this compound on the mitochondrial bioenergetics. Such an increase is difficult to interpret because it could be due to various causes, such as mitochondrial permeability transition pore closing, increased metabolism, etc. [54], which we did not investigate on. It is noteworthy that often an increased mitochondrial potential has been associated to an increased production of reactive oxygen species [55,56], to an early apoptotic phase or to a type of caspase-independent programmed cell death, called necroptosis [55]. All these associated outcomes of increased mitochondrial potential are deleterious for living cells, hampering their normal physiology. Thus, we may affirm that ART 25 and 50 μM impaired normal mitochondrial function. On the contrary, the treatment (24 h) with the analogue EUP induced, at 25 and 50 μM, significant marked mitochondrial depolarization, dramatically increasing the number of round non-apoptotic (mitotic cells) and apoptotic cells (early apoptosis) that appeared together with multinucleated cells [8].

The differences of activity observed between ART and EUP in cancer HeLa cells [8] may be due the difference in methoxylation degrees that distinguish their chemical and biological properties (Table 1). EUP is a chemical analogue of ART, characterized by the absence of the methoxy group at the position 3 of the C ring and the hydroxyl group at the position 7 of the A ring with respect to ART [8]. The lower number of methoxy groups of EUP compared to ART confers to the first flavone a higher hydrophilicity (log P3 = 2.7, Table 1) [10] that partially rises its solubility in the cell medium and possibly influences its mode to interact with the lipid membranes and the mechanism of membrane permeation [5,9].

Conclusions

We presented evidence that ART was inactive against *in vitro* lipid peroxidation but induced a dose-dependent cytotoxicity, lipid profile modulation, and mitochondrial potential increase in

cancer HeLa cells. At the tested dose range, ART seemed to significantly affect metabolic functions of cancer HeLa cells, acting simultaneously through different mechanisms. The insertion of the flavone into the cell membrane lipid bilayer and the effect on membrane fluidity could be the key signal that triggers cells to modify their lipid profile to maintain the physiological cell membrane fluidity. Then the perturbation of membrane lipid organization could therefore affect protein dynamics, with effects on cell viability and increase mitochondrial potential. In conclusion, the capability of ART to modulate structure, composition, and properties of cell membranes is a very promising reality to treat cancer cells that deserves further studies.

Funding sources

This work was supported by the Research Integrative Fund (FIR) of the University of Cagliari to MN - years 2019–2020.

Declaration of Competing Interest

The authors declare no conflict of interest.

References

[1] S. Kumar, A.K. Pandey, Chemistry and biological activities of flavonoids: an overview, ScientificWorldJournal 29 (2013) 162750, https://doi.org/10.1155/2013/162750.

[2] T.-Y. Wang, Q. Li, K.-S. Bi, Bioactive flavonoids in medicinal plants: structure, activity and biological fate, Asian J. Pharm. Sci. 13 (2018) 12–23, https://doi.org/10.1016/j.ajps.2017.08.004.

[3] B. Sengupta, M. Sahihi, M. Dehkhodaei, D. Kelly, I. Arany, Differential roles of 3-hydroxyflavone and 7-hydroxyflavone against nicotine-induced oxidative stress in rat renal proximal tubule cells, PLoS One 12 (2017) e0179777, https://doi.org/10.1371/journal.pone.0179777.

[4] D.M. Kopustinskiene, V. Jakstas, A. Savickas, J. Bernatoniene, Flavonoids as anticancer agents, Nutrients 12 (2020) 457, https://doi.org/10.3390/nu12020457.

[5] V. Abram, B. Berlec, A. Ota, M. Šentjurc, P. Dlatnik, N.P. Ulrih, Effect of flavonoid structure on the fluidity of model lipid membranes, Food Chem. 139 (2013) 804–813, https://doi.org/10.1016/j.foodchem.2013.01.100.

[6] Y. Fang, F. Liang, K. Liu, S. Qaiser, S. Pan, X. Xu, Structure characteristics for intestinal uptake of flavonoids in Caco-2 cells, Food Res. Int. 105 (2018) 353–360, https://doi.org/10.1016/j.foodres.2017.11.045.

[7] Y.S. Tarahovsky, Y.A. Kim, E.A. Yagolnik, E.N. Muzafarov, Flavonoid-membrane interactions: involvement of flavonoid-metal complexes in raft signaling, Biochim. Biophys. Acta 1838 (2014) 1235–1246, https://doi.org/10.1016/j.bbamem.2014.01.021.

[8] A. Rosa, R. Isola, F. Pollastro, P. Caria, G. Appendino, M. Nieddu, The dietary flavonoid eupatilin attenuates in vitro lipid peroxidation and targets lipid profile in cancer HeLa cells, Food Funct. 11 (2020) 5179–5191, https://doi.org/10.1039/D0FO00777C.

[9] A.G. Veiko, S. Sekowski, E.A. Lapshina, A.Z. Wilczewska, K.H. Markiewicz, M. Zamaraeva, Hu-C. Zhao, I.B. Zavodnik, Flavonoids modulate liposomal membrane structure, regulate mitochondrial membrane permeability and prevent erythrocyte oxidative damage, Biochim. Biophys. Acta Biomembr. 1862 (2020) 183442, https://doi.org/10.1016/j.bbamem.2020.183442.

[10] PubChem – NIH, 2021, https://pubchem.ncbi.nlm.nih.gov/#query=2021-58-1.

[11] P. De Souza, A. Gasparotto, S. Crestani, M. Stefanello, M. Marques, C.A Kassuya, Hypotensive mechanism of the extracts and artemetin isolated from *A. millefolium* L. (Asteraceae) in rat, Phytomedicine 18 (2011) 819–825, https://doi.org/10.1016/j.phymed.2011.02.005.

[12] E. Grossini, P. Marotta, S. Farruggio, L. Sigaudo, F. Qoqaiche, G. Raina, V. de Giuli, D. Mary, G. Vacca, F. Pollastro, Effects of artemetin on nitric oxide release and protection against peroxidative injuries in porcine coronary artery endothelial cells, Phytother Res. 29 (2015) 1339–1348, https://doi.org/10.1002/ptr.5386.

[13] A. Gonzalez-Coloma, M. Bailen, C.E. Diaz, B.M. Fraga, R. Martínez-Díaz, G.E. Zuñiga, R.A. Contreras, R. Cabrera, J. Burillo, Major components of Spanish cultivated *Artemisia absinthium* populations: antifeedant, antiparasitic, and antioxidant effects, Ind. Crop. Prod. 37 (2012) 401–407, https://doi.org/10.1016/j.indcrop.2011.12.025.

[14] H.N. Wee, S.Y. Neo, D. Singh, H.-C. Yew, Z.-Y. Qiu, X.-R. C. Tsai, S.-Y. How, K.-Y. C. Yip., C.-H. Tan, H.-L. Koh, Effects of *Vitex trifolia* L. leaf extracts and phytoconstituents on cytokine production in human U937 macrophages, BMC Complement Med. Ther. 20 (2020) 91, https://doi.org/10.1186/s12906-020-02884-w.

[15] D. Lee, C.-E. Kim, S.-Y. Park, K.O. Kim, N.T. Hiep, D. Lee, H.-J. Jang, J.W. Lee, K.S. Kang, Protective effect of *Artemisia argyi* and its flavonoid constituents against contrast-Induced cytotoxicity by iodixanol in LLC-PK1 cells, Int. J. Mol. Sci. 19 (2018) 1387, https://doi.org/10.3390/ijms19051387.

[16] V.K. Sridevi, H.S. Chauhan, N.K. Singh, S.K. Singh, Antioxidant and hepatoprotective effects of ethanol extract of *Vitex glabrata* on carbon tetrachloride-induced liver damage in rats. Nat. Prod. Res. 26 (2012) 1135–1140, https://doi.org/10.1080/14786419.2011.560849.

[17] A. Martins, R. Mignon, M. Bastos, D. Batista, N.R. Neng, J.M. Nogueira, C. Vizetto-Duarte, L. Custódio, J. Varela, A.P. Rauter, In vitro antitumoral activity of compounds isolated from *Artemisia gorgonum* Webb, Phytother. Res. 28 (2014) 1329–1334, https://doi.org/10.1002/ptr.5133.

[18] M.C. Bayeux, A.T. Fernandes, M.A. Foglio, J.E. Carvalho, Evaluation of the antiedematogenic activity of artemetin isolated from *Cordia currassavica* DC., Braz. J.

Med. Biol. Res. 35 (2002) 1229–1232, https://doi.org/10.1590/S0100-879X2002001000017.

[19] B. Csupor-Löffler, Z. Hajdú, I. Zupkó, B. Réthy, G. Falkay, P. Forgo, J. Hohmann, Antiproliferative effect of flavonoids and sesquiterpenoids from *Achillea millefolium* s.l. on cultured human tumour cell lines, Phytother. Res. 23 (2009) 672–676, https://doi.org/10.1002/ptr.2697.

[20] D. Casares, P. V. Escribá, C. A. Rosselló, Membrane lipid composition: effect on membrane and organelle structure, function and compartmentalization and therapeutic avenues, Int. J. Mol. Sci. 20 (2019) 2167, https://doi.org/10.3390/ijms20092167.

[21] G. Barrera, Oxidative stress and lipid peroxidation products in cancer progression and therapy, ISRN Oncol. 2012 (2012) 137289, https://doi.org/10.5402/2012/137289.

[22] S. Petrovic, A. Arsic, D. Ristic-Medic, Z. Cvetkovic, V. Vucic, Lipid peroxidation and antioxidant supplementation in neurodegenerative diseases: A review of human studies, Antioxidants 9 (2020) 1128, https://doi.org/10.3390/antiox9111128.

[23] Q. Liu, Q. Luo, A. Halim, G. Song, Targeting lipid metabolism of cancer cells: A promising therapeutic strategy for cancer, Cancer Lett. 401 (2017) 39–45, https://doi.org/10.1016/j.canlet.2017.05.002.

[24] V. Lladó, D. J. López, M. Ibarguren, M. Alonso, J.B. Soriano, P.V. Escribá, X. Busquets, Regulation of the cancer cell membrane lipid composition by NaCHOleate. Effects on cell signaling and therapeutical relevance in glioma, Biochim. Biophys. Acta 1838 (2014) 1619–1627, https://doi.org/10.1016/j.bbamem.2014.01.027.

[25] A. Rosa, D. Caboscio, R. Isola, M. Nieddu, G. Appendino, A.M. Falchi, Dietary zerumbone from shampoo ginger: new insights into its antioxidant and anticancer activity, Food Funct. 10 (2019) 1629–1642, https://doi.org/10.1039/C8FO02395F.

[26] Z. Tracz-Gaszewska, P. Dobrzyn, Stearoyl-CoA desaturase 1 as a therapeutic target for the treatment of cancer, Cancers (Basel) 11 (2019) 948, https://doi.org/10.3390/cancers11070948.

[27] J.S. Zhang, J.P. Lei, G.Q. Wei, H. Chen, C.Y. Ma, H.Z. Jiang, Natural fatty acid synthase inhibitors as potent therapeutic agents for cancers: A review, Pharm. Biol. 54 (2016) 1919–1925, https://doi.org/10.3109/13880209.2015.1113995.

[28] G. Appendino, O. Taglialatela-Scafati, A. Romano, F. Pollastro, C. Avonto, P. Rubiolo, Genepolide, a sesterpene-γ-lactone with a novel carbon skeleton from mountain wormwood (*Artemisia umbelliformis*), J. Nat. Prod. 73 (2009) 340–344, https://doi.org/10.1021/np800468m.

[29] A.J. Falk, S.J. Smolenski, L. Bauer, C.L. Bell, Isolation and identification of three new flavones from *Achillea millefolium* L., J. Pharm. Sci. 64 (1975) 1838–1842.

[30] A. Rosa, A. Atzeri, M. Nieddu, G. Appendino, New insights into the antioxidant activity and cytotoxicity of arzanol and effect of methylation on its biological properties, Chem. Phys. Lipids 205 (2017) 55–64, https://doi.org/10.1016/j.chemphyslip.2017.05.001.

[31] A. Rosa, S. Murgia, D. Putzu, V. Meli, A.M. Falchi, Monoolein-based cubosomes affect lipid profile in HeLa cells, Chem. Phys. Lipids 191 (2015) 96–105, https://doi.org/10.1016/j.chemphyslip.2015.08.017.

[32] J.Y. Kim, S.H. Shim, Anti-atherosclerotic effects of fruits of Vitex rotundifolia and their isolated compounds via inhibition of human LDL and HDL oxidation, Biomolecules 9 (2019) 727, https://doi.org/10.3390/biom9110727.

[33] A.M. Falchi, A. Rosa, A. Atzeri, A. Incani, S. Lampis, V. Meli, C. Caltagirone, S. Murgia, Effects of monoolein-based cubosome formulations on lipid droplets and mitochondria of HeLa cells, Toxicol. Res. 4 (2015) 1025–1036, https://doi.org/10.1039/c5tx00078e.

[34] C. Garenc, P. Julien, E. Levy, Oxysterols in biological systems: the gastrointestinal tract, liver, vascular wall and central nervous system, Free Rad. Res. 44 (2010) 47–73, https://doi.org/10.3109/10715760903321804.

[35] R. Amorati, A. Bacchieri, A. Cowden, L. Valgimigli, The antioxidant activity of quercetin in water solution, Biomimetics (Basel) 2 (2017) 9, https://doi.org/10.3390/biomimetics2030009.

[36] M. Mosca, A. Ceglie, L. Ambrosone, Effect of membrane composition on lipid oxidation in liposomes, Chem. Phys. Lipids 164 (2011)158–165, https://doi.org/10.1016/j.chemphyslip.2010.12.006.

[37] A.J. Jr. Dugas, J. Castañeda-Acosta, G.C. Bonin, K.L. Price, N.H. Fischer, G.W. Winston, Evaluation of the total peroxyl radical-scavenging capacity of flavonoids: structure-

activity relationships, J. Nat. Prod. 63 (2000) 327–331, https://doi.org/10.1021/np990352n.

[38] J. Hu, W. Ma, L.N. Wei, K.-J. Wang, Antioxidant and anti-inflammatory flavonoids from the flowers of Chuju, a medical cultivar of *Chrysanthemum morifolim* Ramat, J. Mex. Chem. Soc. 61 (2017) 282–289, http://www.scielo.org.mx/scielo.php?script=sci_arttext&pid=S1870-249X2017000400282&lng=es&nrm=iso.

[39] V. Fritz, Z. Benfodda, C. Henriquet, S. Hure, J.P. Cristol, F. Michel, M.A. Carbonneau, F. Casas, L. Fajas, Metabolic intervention on lipid synthesis converging pathways abrogates prostate cancer growth, Oncogene 32 (2013) 5101–5110, https://doi.org/10.1038/onc.2012.523.

[40] X. Luo, C. Cheng, Z. Tan, N. Li, M. Tang, L. Yang, Y. Cao, Emerging roles of lipid metabolism in cancer metastasis, Mol. Cancer. 16 (2017) 76, https://doi.org/10.1186/s12943-017-0646-3.

[41] C.R. Santos, A. Schulze, Lipid metabolism in cancer, FEBS J. 279 (2012) 2610-2623,

[42] J.F. Ferreira, D.L. Luthria, T. Sasaki, A. Heyerick, Flavonoids from *Artemisia annua* L. as antioxidants and their potential synergism with artemisinin against malaria and cancer, Molecules 15 (2010) 3135–3170, https://doi.org/10.1111/j.1742-4658.2012.08644.x.

[43] W.G. Ko, T.H. Kang, S.J. Lee, N.Y. Kim, Y.C. Kim, D.H. Sohn, B.H. Lee, Polymethoxyflavonoids from *Vitex rotundifolia* inhibit proliferation by inducing apoptosis in human myeloid leukemia cells, Food Chem. Toxicol. 38 (2000) 861–865, https://doi.org/10.1016/S0278-6915(00)00079-X.

[44] J. Kobayakawa, Y. Sato-Nishimori, M. Moriyasu, Y. Matsukawa, G2-M arrest and antimitotic activity mediated by casticin, a flavonoid isolated from Viticis Fructus (*Vitex rotundifolia* Linne fil.), Cancer Lett. 208 (2004) 59–64, https://doi.org/10.1016/j.canlet.2004.01.012.

[45] Y.A. Kim, H. Kim, Y. Seo, Antiproliferative effect of flavonoids from the halophyte *Vitex rotundifolia* on human cancer cells, Nat. Prod. Commun. 8 (2013) 1405–1408, https://doi.org/10.1177/1934578X1300801016.

[46] W.X. Li, C.B. Cui, B. Cai, H.Y. Wang, X.S. Yao, Flavonoids from *Vitex trifolia* L. inhibit cell cycle progression at G2/M phase and induce apoptosis in mammalian cancer cells, J.

Asian. Nat. Prod. Res. 7 (2005) 615–626, https://doi.org/10.1080/10286020310001625085.

[47] L. Gibellini, M. Pinti, M. Nasi, J.P. Montagna, S. De Biasi, E. Roat, L.Bertoncelli, E.L. Cooper, A. Cossarizza, Quercetin and cancer chemoprevention, Evid. Based Complement. Alternat. Med. (2011) 2011, 591356, https://doi.org/10.1093/ecam/neq053.

[48] M.K. Dymond, C.V. Hague, A.D. Postle, G. S. Attard, An in vivo ratio control mechanism for phospholipid homeostasis: evidence from lipidomic studies, J. R. Soc. Interface 10 (2012) 20120854, https://doi.org/10.1098/rsif.2012.0854.

[49] P.C. Theodoropoulos, S.S. Gonzales, S.E. Winterton, C. Rodriguez-Navas, J.S. McKnight, L.K. Morlock, J.M. Hanson, B. Cross, A.E. Owen, Y. Duan, J.R. Moreno, A. Lemoff, H. Mirzaei, B.A. Posner, N.S. Williams, J.M. Reddy, D. Nijhawan, Discovery of tumor-specific irreversible inhibitors of stearoyl CoA desaturase, Nat. Chem. Biol. 12 (2016) 218–225, https://doi.org/10.1038/nchembio.2016.

[50] G. Maulucci, O. Cohen, B. Daniel, A. Sansone, P.I. Petropoulou, S. Filou, A. Spyridonidis, G. Pani, M. De Spirito, S. Chatgilialoglu, C. Ferreri, K.E. Kypreos, S. Sasson, Fatty acid-related modulations of membrane fluidity in cells: detection and implications. Free Radic. Res. 50 (sup1) (2016) S40–S50, https://doi.org/10.1080/10715762.2016.1231403.

[51] H. Strahl, F. Bürmann, L. W. Hamoen, The actin homologue MreB organizes the bacterial cell membrane, Nat. Commun. 5 (2014) 3442, https://doi.org/10.1038/ncomms4442.

[52] S. Selvaraj, S. Krishnaswamy, V. Devashya, S. Sethuraman, U.M. Krishnan, Influence of membrane lipid composition on flavonoid-membrane interactions: Implications on their biological activity, Prog. Lipid Res. 58 (2015) 1–13, https://doi.org/10.1016/j.plipres.2014.11.002.

[53] G. Preta, New insights into targeting membrane lipids for cancer therapy, Front. Cell Dev. Biol. 8 (2020) 876, https://doi.org/10.3389/fcell.2020.571237.

[54] L.D. Zorova, V.A. Popkov, E.Y. Plotnikov, D.N. Silachev, I.B. Pevzner, S.S. Jankauskas, V.A. Babenko, S.D. Zorov, A.V. Balakireva, M. Juhaszova, S.J. Sollott, D.B. Zorov, Mitochondrial membrane potential, Anal. Biochem. 552 (2018) 50–59, https://doi.org/10.1016/j.ab.2017.07.009.

[55] G. Warnes, Flow cytometric detection of hyper-polarized mitochondria in regulated and accidental cell death processes, Apoptosis 25 (2020) 548–557, https://doi.org/10.1007/s10495-020-01613-5.

[56] P. Jr. Gergely, B. Niland, N. Gonchoroff, R. Jr. Pullmann, P.E. Phillips A. Perl, Persistent mitochondrial hyperpolarization, increased reactive oxygen intermediate production, and cytoplasmic alkalinization characterize altered IL-10 signaling in patients with systemic lupus erythematosus, J. Immunol. 169 (2002) 1092–1101, http://www.jimmunol.org/content/169/2/1092.

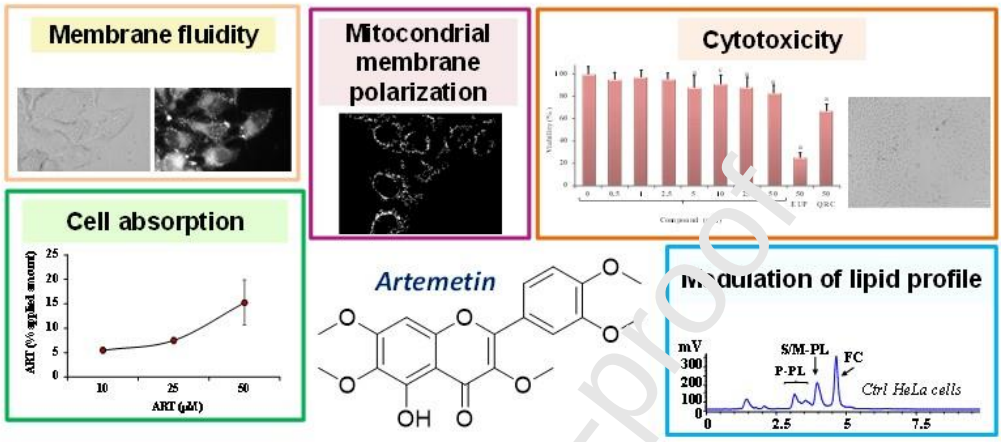

CRediT author statement

A. Rosa designed the experiments, participated in the experimental work and data analysis, wrote the original manuscript draft, revised and edited the manuscript. R. Isola, F. Pollastro, and M. Nieddu participated in the experimental work and data analysis, read and approved the final manuscript. All authors discussed the experiments results and contributed to the final manuscript.

Declaration of interests

X The authors declare that they have no known competing financial interests or personal relationships that could have appeared to influence the work reported in this paper.

☐The authors declare the following financial interests/personal relationships which may be considered as potential competing interests: